ZINC(II) FERROCENYLTHIOSEMICARBAZONE COMPLEXES: STRUCTURE, ELECTROCHEMISTRY, DNA BINDING AND NUCLEASE ACTIVITY

VIKNESWARAN A/L RAJAMUTHY

UNIVERSITI SAINS MALAYSIA

August 2011

ZINC(II) FERROCENYLTHIOSEMICARBAZONE COMPLEXES: STRUCTURE, ELECTROCHEMISTRY, DNA BINDING AND NUCLEASE ACTIVITY

by

VIKNESWARAN A/L RAJAMUTHY

Thesis submitted in fulfilment of the
requirements for the degree of
Master of Science

August 2011

ACKNOWLEGDEMENT

I would like to express my sincere appreciation to my supervisor Prof. Teoh Siang Guan, for guiding my work with greatest concern and providing me with knowledge and experiences beyond my expectations. As a supervisor you have always been available and supportive. You have been an excellent supervisor providing encouragement, expert advice and criticism. Without your support and continuous encouragement, my work would not have been completed on time.

I would also like to thank my co supervisor Dr Amin Malik Shah Abdul Majid for his guidance and advice on DNA binding experiments. Thanks as well to Prof. Fun Hoong Kun for help regarding X-ray crystallography. My sincere gratitude also goes to the Dean, lecturers and supporting staffs of the School of Chemical Sciences for their support and assistance throughout my candidature.

Last but not least, to my parents, Mr. Rajamuthy and Mdm. Puspharani, thank you so much for your love, support and patience.

TABLE OF CONTENT

LIST OF TABLES

LIST OF FIGURES

LIST OF FIGURE

ZINK(II) FEROSENILTIOSEMIKARBAZON KOMPLEKS: STRUKTUR, ELEKTROKIMIA, PENGIKATAN DNA DAN AKTIVITI NUKLEASA

ABSTRAK

Empat zink kompleks yang berformula $Zn\{(\eta^5\text{-}C_5H_5)Fe(\eta^5\text{-}C_5H_4)C(H)=NN=C(S)NH_2\}_2$ (**V**), $Zn\{(\eta^5\text{-}C_5H_5)Fe(\eta^5\text{-}C_5H_4)C(H)=NN=C(S)N(H)CH_3\}_2\cdot CH_3OH$ (**VI**), $Zn\{(\eta^5\text{-}C_5H_5)Fe(\eta^5\text{-}C_5H_4)C(H)=NN=C(S)N(H)C_2H_5\}_2$ (**VII**), $Zn\{(\eta^5\text{-}C_5H_5)Fe(\eta^5\text{-}C_5H_4)C(H)=NN=C(S)N(H)C_6H_5\}_2\cdot H_2O$ (**VIII**) disintesis dan dicirikan. Struktur kompleks ini telah ditentukan melalui analisis pembelauan sinar-X hablur tunggal. Geometri koordinatan zink dalam kompleks ini adalah sama iaitu pengkoordinatan tetrahedron terherot. Kompleks ini adalah redoks aktif dengan memberi sambutan voltametri berkitar untuk gandingan Fe(III) − Fe(II) pada keupayaan hampir 0.5 V vs. Ag/AgCl. Pemalar pengikatan, K_b bagi kompleks untuk mengikat CT DNA adalah dalam julat 7.0×10^2 hingga 4.8×10^3 M^{-1}. Kompleks ini tidak menyisip ke dalam nukliobes CT DNA sepertimana dijelaskan oleh pengukuran kelikatan. Mereka mempamerkan aktiviti nukleasa yang efisien tanpa kehadiran agen pengaktifan dengan membelah 'supercoil' DNA ke bentuk 'nicked' dan 'linear' pada kepekatan yang rendah.

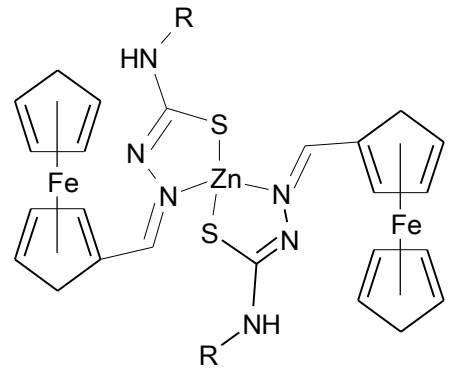

R = H, **V**; CH_3, **VI**; C_2H_5, **VII**; C_6H_5, **VII**

ZINC(II) FERROCENYLTHIOSEMICARBAZONE COMPLEXES: STRUCTURE, ELECTROCHEMISTRY, DNA BINDING AND NUCLEASE ACTIVITY

ABSTRACT

Four zinc complexes of the formulae $Zn\{(\eta^5\text{-}C_5H_5)Fe(\eta^5\text{-}C_5H_4)C(H)=NN=C(S)NH_2\}_2$ (**V**), $Zn\{(\eta^5\text{-}C_5H_5)Fe(\eta^5\text{-}C_5H_4)C(H)=NN=C(S)N(H)CH_3\}_2\cdot CH_3OH$ (**VI**), $Zn\{(\eta^5\text{-}C_5H_5)Fe(\eta^5\text{-}C_5H_4)C(H)=NN=C(S)N(H)C_2H_5\}_2$ (**VII**), $Zn\{(\eta^5\text{-}C_5H_5)Fe(\eta^5\text{-}C_5H_4)C(H)=NN=C(S)N(H)C_6H_5\}_2\cdot H_2O$ (**VIII**) have been synthesised and characterised. The structures of these complexes have been established by a single-crystal X-ray diffraction analysis. The coordination geometries of the zinc centres are identical, showing a distorted tetrahedral coordination. The complexes are redox active, giving a reversible cyclic voltammetric response of the Fe(III) − Fe(II) couple near 0.5 V vs. Ag/AgCl. The binding constants, K_b, of the complexes for binding with CT DNA are in the range of 7.0×10^2 to 4.8×10^3 M^{-1}. The complexes do not intercalate into the nucleobases of CT DNA as evident from viscosity measurements. They exhibit efficient nuclease activity in the absence of an activating agent by cleaving supercoiled DNA into nicked and linear forms of DNA at low concentrations.

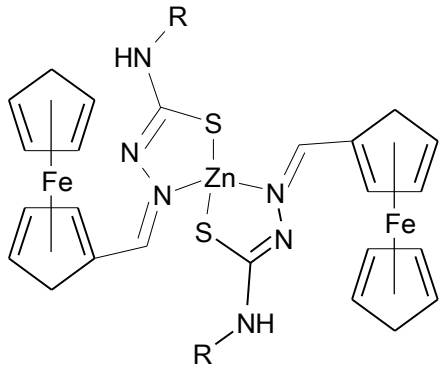

R = H, **V**; CH_3, **VI**; C_2H_5, **VII**; C_6H_5, **VII**

1 INTRODUCTION

1.1 History of Metallodrugs

Medicinal applications of metallic elements have been practised for almost 5000 years (Sadler & Sykes, 1991). As far back as 3000 BC, the Egyptians used copper to sterilise water. Gold was used in a variety of medicines in Arabia and China 3500 years ago. Various iron remedies were used in Egypt about 1500 BC, around the same time that zinc was discovered to promote the healing of wounds. In Renaissance era Europe, mercurous chloride was used as a diuretic and the nutritional essentiality of iron was discovered. It is in the last 100 years, however, that the medicinal activity of inorganic compounds has slowly been developed in a rational manner, starting in the early 1900s with $K[Au(CN)_2]$ for tuberculosis, antimony compounds for leishmaniasis, silver nitrate for epilepsy and various gold salts to treat bacterial infectious diseases (Fung & Bowen, 1996; Orvig & Abrams, 1999; Tripathi, 2009).

1.2 DNA is primary target of metal-based anti-cancer drug cisplatin

The modern medicinal inorganic chemistry gains much attention since the discovery of *cis*-diamminedichloroplatinum(II), or cisplatin (Kelland, 2007). One of the most successful drugs in modern pharmacology, cisplatin, had been known since 1845, but its antitumour was only established in 1970. Cisplatin has been used to treat various cancer diseases namely ovarian, cervical, head and neck, oesophageal, and non-small cell lung cancer (Kroep *et al.*, 1999). Much research has been conducted over the 30 years following the discovery of biological activity for cisplatin in the attempt to elucidate its mechanism of action. Many cellular components including DNA, RNA, proteins, membrane phospholipids and actin

filaments are potential targets for cisplatin. The first clue for identifying the primary cellular target was the filamentous growth (Figure 1.1) of the bacteria induced by cisplatin, an occurrence characteristic of DNA-damaging agents such as ionizing radiation, UV radiation and hydroxyurea (Adler & Hardigree, 1965; Rosenkranz, Garro, Levy, & Carr, 1966; Witkin, 1967). Cisplatin treatment also led to lysis of *Escherichia coli* cells containing bacteriophage λ, another occurrence characteristic of DNA-damaging agent (Reslova, 1971). These early experiments pointed to DNA as an important cellular target. Lippard and co-workers have elucidated the detailed molecular mechanism of action, which involves covalent binding of cisplatin to DNA (Jamieson & Lippard, 1999).

Figure 1.1: An example of filamentous growth of the bacteria induced by DNA damaging agents. Nuclear material appears as bright body (Adler & Hardigree, 1965).

1.3 Rational on designing zinc(II) ferrocenylthiosemicarbazone

In common with many other anti-cancer drugs (Abdullah *et al.*, 2006; Chari, 2007; Kunwar *et al.*, 2008; Maeda, Bharate, & Daruwalla, 2009), cisplatin induces normal tissue toxicity (Rowan, 2010; Srivastava *et al.*, 1996). So, attempts are being made to replace this drug with non-toxic, efficacious, and target-specific noncovalently DNA binding anticancer drugs. Generally anticancer agents that are

approved for clinical use are molecules which damage DNA, block DNA synthesis indirectly through inhibition of nucleic acid precursor biosynthesis, or disrupt hormonal stimulation of cell growth (Foye, 1995). Therefore, considerable effort has been now focused on the development of new anticancer drugs based on transition metal complexes, particularly, biocompatible complexes, that bind to and cleave DNA under physiological conditions. Among many metal ions, zinc(II) has aroused our attention due a variety of factors, zinc(II) is a good Lewis acid, exchanges ligands rapidly and is not toxic. Both the former are requirements for a metal ion to be an effective hydrolytic DNA cleaver (Mancin & Tecilla, 2007). Further, zinc(II) has no ligand field stabilization energy and, as a consequence, it can easily adapt its coordination geometry to best fulfil the structural requirement of a DNA hydrolysis reaction (Mancin & Tecilla, 2007). In 2004, Bazzicalupi and co-workers reported a binuclear zinc complex $[Zn_2L_2(OH)_2]_2^{2+}$, where L is 2,5,8,11,14-Pentaaza[15]-[15](2,2‘)[1,15]-bipyridylophane (**1**) that hydrolyses the phosphate ester bond of bis(*p*-nitrophenyl)phosphate (**2**). They pointed out that the hydrolytic pathway is a concerted process (single step) where there is bridging interaction of the substrate with the two zinc(II) ions and nucleophilic attack of a Zn-OH function at phosphorus (Bazzicalupi *et al.*, 2004).

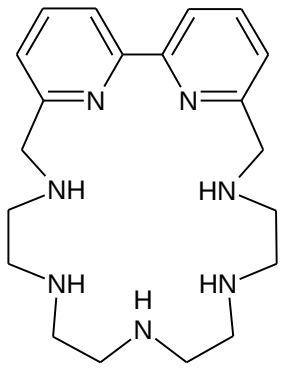

1

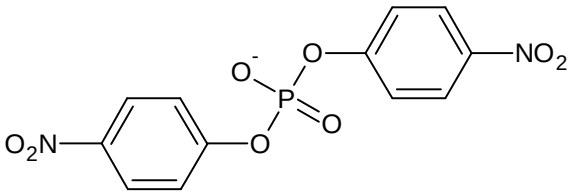

2

In 2006, Ibrahim showed bridged μ-hydroxo zinc(II) complex [TtiZn(μOH)ZnTti]ClO_4 (**3**), where Tti is hydrotris(*N*-xylyl-2-thioimidazolyl)borate (**4**) cleaves the P-O bond in tris(*p*-nitrophenyl)phosphate (**5**) to form a mixture of a monomeric phosphate diester complex and phenoxo complex (Ibrahim, 2006).

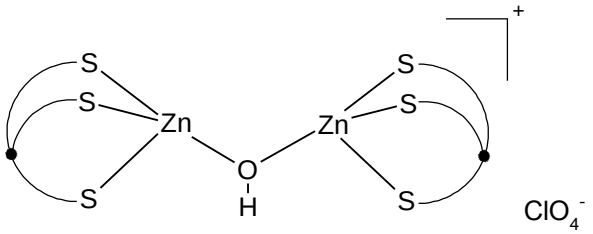

3

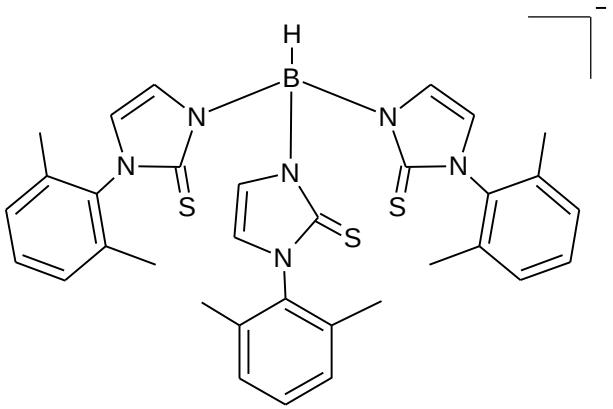

4

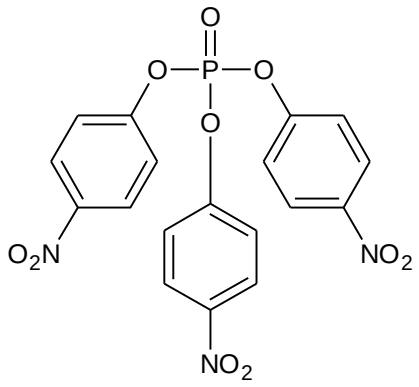

5

This is the first example of zinc-mediated hydrolysis with S_3 in the coordination sphere capable of promoting phosphoester hydrolysis. The cleavage mechanism proposed by the author is shown in Scheme 1.1.

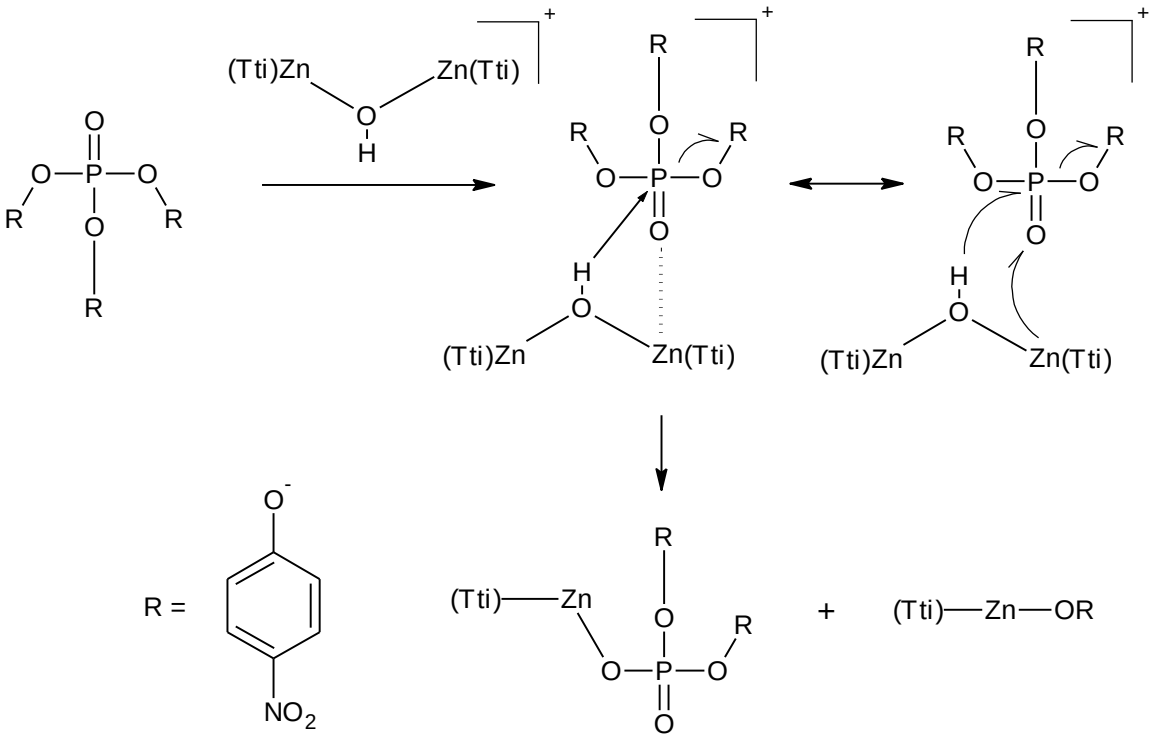

Scheme 1.1: The proposed mechanism for the hydrolytic cleavage of tris(*p*-nitrophenyl)phosphate by [TtiZn(μOH)ZnTti]ClO_4 (Ibrahim, 2006).

Molecules that can hydrolyse phosphodiester bond are potential Topoisomerase inhibitors (Wang, Wang, Kingsbury, Johnson, & Hecht, 1998). Topoisomerase inhibitors are quoted as having a wide range of antitumour activities and are among the most widely used anticancer drugs clinically (Beretta, Perego, & Zunino, 2008; Pommier, 2006; Rothenberg, 1997; Sunami *et al.*, 2009; Teicher, 2008). Topoisomerase I and II are enzymes that bind to supercoiled DNA, forming a cleavable complex and through strand breakage, passage and re-ligation allow a wide variety of essential DNA metabolic reactions including replication and repair to take place. These enzymes are functionally related, work together and appear to be essen-

tial to maintain cellular viability throughout the cell cycle (Rothenberg, 1997). Topotecan, a topoisomerase I inhibitor anti cancer agent exerts its cytotoxic effects by stabilizing the covalent DNA-topoisomerase I cleavable complex. When DNA replicates in the presence of this complex, double-strand breaks occur and the resulting DNA fragmentation causes cell death (Staker *et al.*, 2002). Very recently, Seng and co-workers observed [Zn(3-Me-pic)$_2$(phen)] (**6**) where 3-Me-pic is 3-methyl-picolinate and phen is 1,10-phenanthroline, can inhibit the function of topoisomerase I. Preliminary investigation shows the complex is antiproliferative against MCF-7 breast cancer cells with an IC_{50} value of 4.8 μM (Seng *et al.*, 2009).

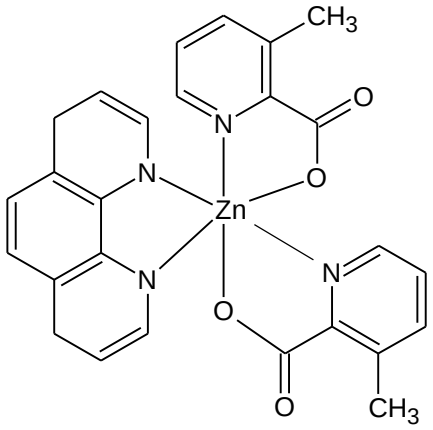

6

Metal complexes that able to cleave DNA upon photoactivation under physiological conditions have also received considerable attention because of their possible utility in highly targeted photodynamic therapeutic applications (Armitage, 1998; Boerner & Zaleski, 2005; Bradley, Angeles-Boza, Dunbar, & Turro, 2004). Photodynamic therapy (PDT) has emerged as a viable alternative mode of treatment of cancer (Ali & van Lier, 1999; Detty, Gibson, & Wagner, 2004; Sternberg, Dolphin, & Brückner, 1998). PDT is based on the concept that certain therapeutic molecules called photosensitisers (PS) can be preferentially localised in malignant

tissues, and when these PSs are activated with appropriate wavelength of light, they pass on their excess energy to surrounding molecular oxygen, resulting in the generation of reactive oxygen species (ROS), such as free radicals and singlet oxygen ($^1O_2$), which are toxic to cells and tissues. PDT is a non-invasive treatment and used for several types of cancers, and its advantage lies in the inherent dual selectivity. First, selectivity is achieved by a preferential localization of the photosensitiser in target tissue (e.g., cancer), and second, the photoirradiation and subsequent photodynamic action can be limited to a specific area of interest. Because the PS is non-toxic without light exposure, only the irradiated areas will be affected, even if the PS does infiltrate normal tissues. Selectivity can be further enhanced by combining the PS with molecular delivery systems or by conjugating PS's with targeting agents such as an integrin antagonist or carbohydrates, which have high affinity for cancer tissue (Ohulchanskyy *et al.*, 2007). In 2002, Ishikawa and co-workers prepared zinc complexes of cationic bis-porphyrins composed of two H_2TMPyP *meso*-tetrakis(*N*-methyl-4-pyridyl)porphine linked with a series of aliphatic diamines (**7**) to improve less DNA photocleavage activities of the metal-free bis-porphyrins. The poor activities seemed to be derived from their intermolecular aggregation properties in aqueous solution. Zinc(II) insertion into the metal-free cationic bis-porphyrins fully enhanced their DNA photocleavage activities by 3 fold (Ishikawa, Yamakawa, & Uno, 2002). In 2007, Ishikawa and co-workers showed that zinc(II) complexes with two TMPyP chromophores bridged by *para*- or *meta*-xylylenediamine (**8**) have potent photocleavage activity. The xylylene linkers and zinc ion were introduced to control interchromophoric interaction that involved in photosensitization of the cationic bis-porphyrins (Ishikawa, Yamakawa, & Uno, 2007).

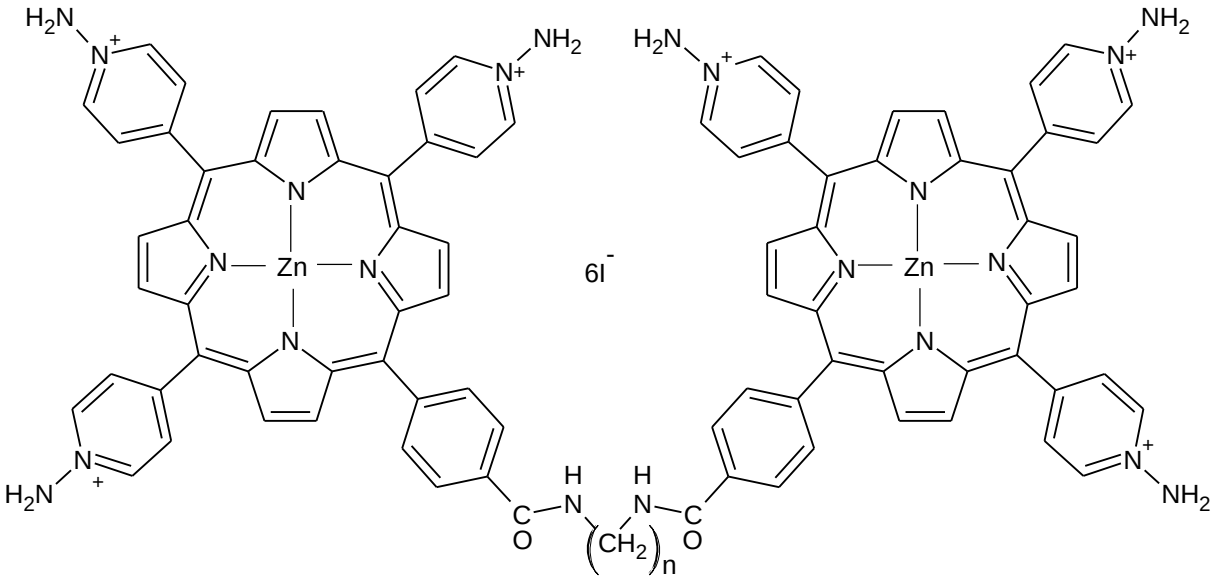

n = 2, 6, 10

7

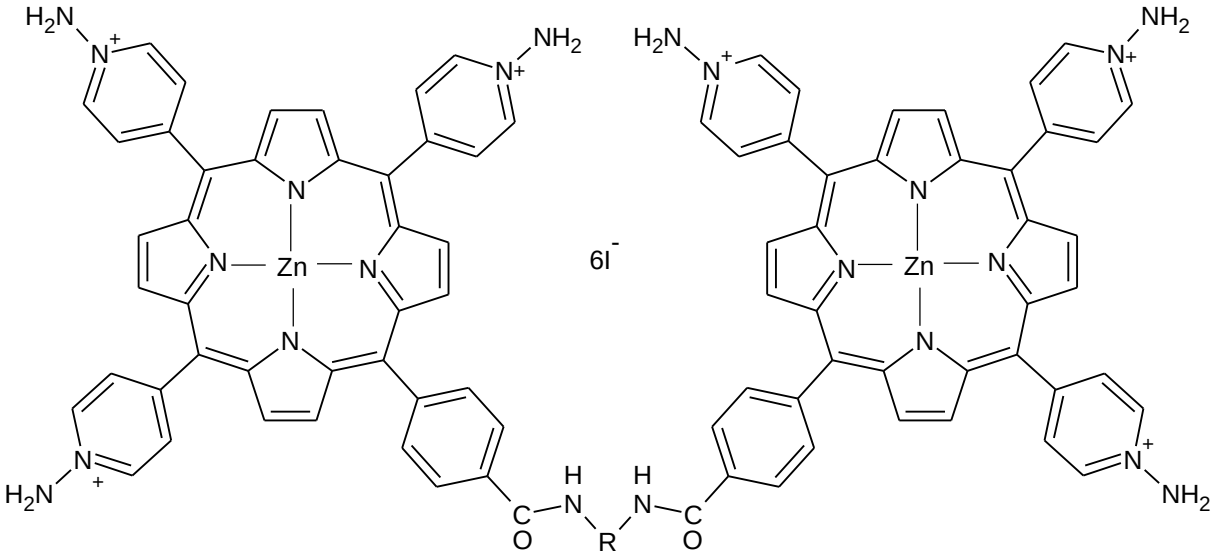

R = 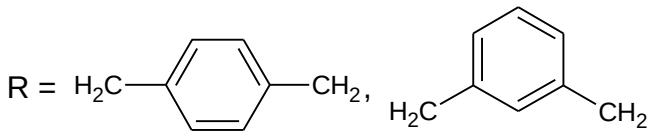

8

Pharmacological behaviour of a metal complex also depends on the ligand framework. In designing the zinc(II) complexes, we have chosen ferrocene conjugated to thiosemicarbazone chain. Among different organometallic systems, those based on ferrocene and its conjugates are of particular importance for their medicinal activity due to excellent stability of the ferrocene moiety in biological media, its lipophilicity, and its reversible redox chemistry. In addition, ferrocene could readily form a variety of stable conjugate species (Maity, Roy, Saha, & Chakravarty, 2009), for example, anticancer and antimalarial drugs, namely, ferrocifen (ferrocene-conjugated tamoxifen) (**9**) and ferroquine (ferrocene-attached chloroquine) (**10**) (Biot, 2004; Biot *et al.*, 1997; Jaouen, Top, VessiÃ¨res, Leclercq, & McGlinchey, 2004). It has been reported that the cytotoxicity of tamoxifen is greatly enhanced due to the presence of a ferrocenyl moiety (Fc = $(\eta^5\text{-}C_5H_4)Fe^{II}(\eta^5\text{-}C_5H_5)$) showing activity against oestrogen-dependent and oestrogen-independent breast cancer cells (Jaouen *et al.*, 2004). In the case of chloroquine, the ferrocenyl moiety strongly influences the antimalarial activity (Biot, 2004; Biot *et al.*, 1997).

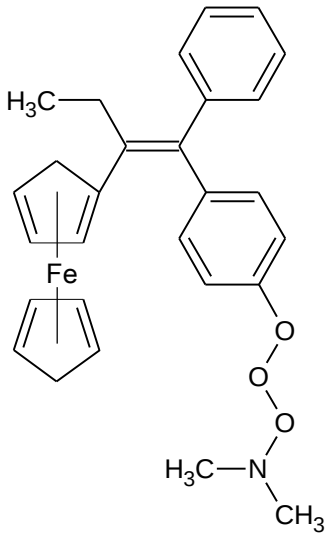

9

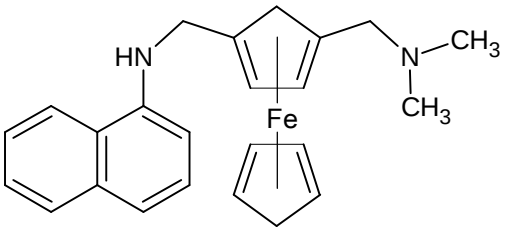

10

In a latest report, when phenyl is replaced with ferrocene in the complex [Cu(Ph-tpy)(dppz)]$(ClO_4)_2$ (**11**), where Ph-tpy is 4′-phenyl-2,2′:6′,2″-terpyridine and dppz is dipyridophenazine, the complex showed better photocytotoxicity against Hela cells (Maity *et al.*, 2010).

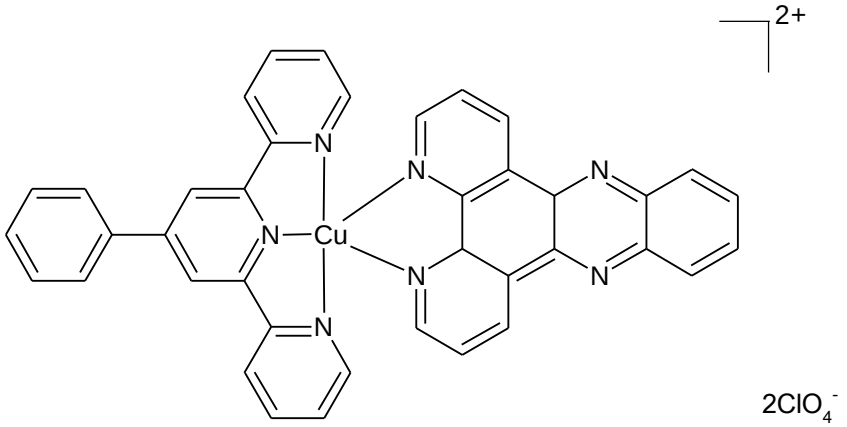

11

On the other hand, thiosemicarbazone is a bio-multiutility N, S-donor ligand. Thiosemicarbazones can be obtained by a simple condensation reaction of an aldehyde or a ketone with a thiosemicarbazide, and are broadly classified as mono-thiosemicarbazones and bis-thiosemicarbazones. The basic mono-thiosemicarbazone ligand has different, R^1, R^2, R^3 and R^4 substituents, and depending upon the substituents, various sub-classes of ligands are formed. Thiosemicabazones based on aldehydes (e.g., **12**) have hydrogen atom as one of the substituents (R^2) at C^2 carbon, while second substituent R^1 may be an alkyl, an aryl or a heterocyclic group. Similarly, substituents at N^1 nitrogen may be both hydrogen atoms, or one hydrogen, and second alkyl, or aryl group, and finally N^1 may be a part of the cyclic ring.

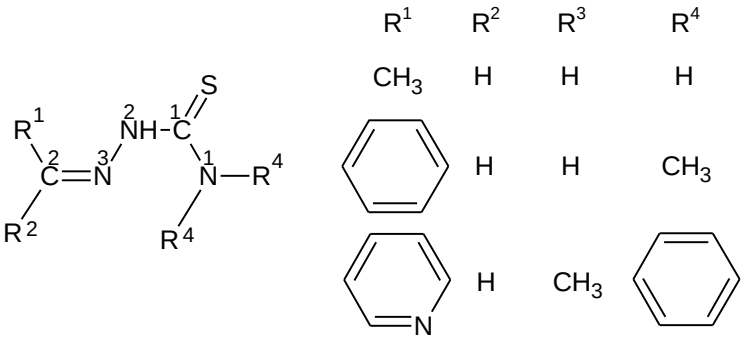

12

The second category, bis-thiosemicarbazones have two arms connected *via* a ring (**13**) or a C-C bond (**14**) (Lobana, Sharma, Bawa, & Khanna, 2009).

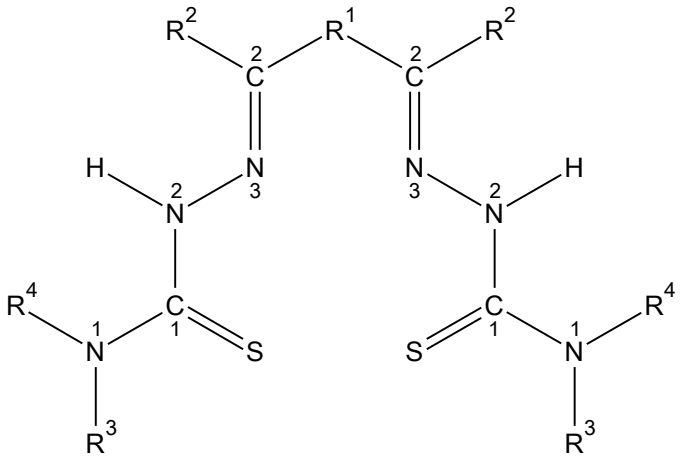

13

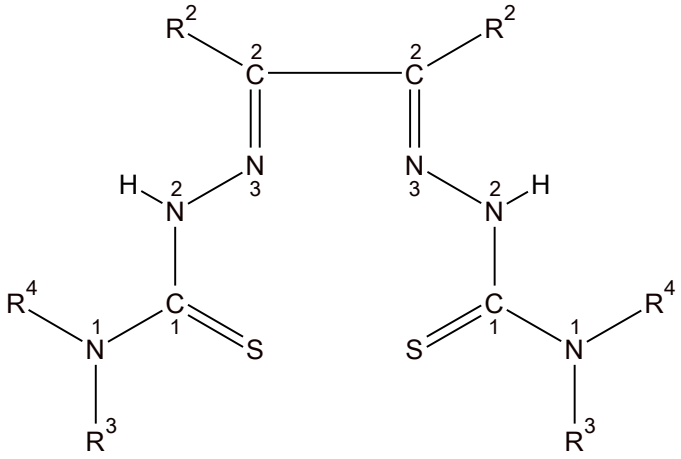

14

Thiosemicarbazones (TSC) possess a wide range of biological activity depending on the parent aldehyde or ketone. Brockman and co-workers first showed that 2-formylpyridine TSC possesses antileukaemic activity in mice bearing leukaemic cells (Brockman, Thomson, J, & Skipper, 1956). Following this initial report, a large series of TSCs derived from 2-formylpyridines, isoquinoline-1 carboxaldehydes, and 2-acetylpyridine were synthesised and their *in vivo* antitumour activity were evaluated. Among the derivatives, 5-hydroxypyridine TSC (**15**), which showed significant antitumour activity has been selected for clinical phase I evaluation (Agrawal & Sartorelli, 1978; Scovill, Klayman, & Franchino, 1982).

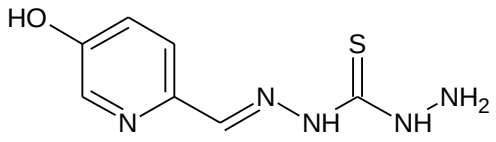

15

In 2001, Easmon and co-workers reported a series of thiosemicarbazones bearing a N-azabicyclo[3.2.2]nonane moiety derived from 3-acylpyridazines (**16**), 4-acetylpyrimidines (**17**), and 2-acetylpyrazines (**18**) exhibits cytotoxic activity against human acute lymphoblastic leukaemia CCRF-CEM cells (IC_{50} = 0.05 – 0.77 μM) and colon adenocarcinoma HT-29 cells (IC_{50} = 0.011 – 2.22 μM) (Easmon *et al.*, 2001).

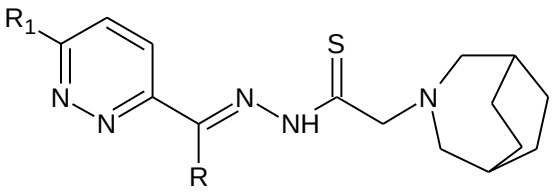

R = CH_3, R^1 = H

R = CH_3, R^1 = CH_3

R = CH_2CH_3, R^1 = H

16

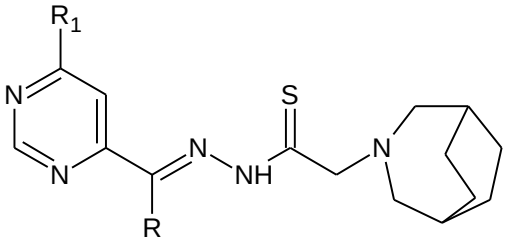

R = CH_3, R^1 = H

R = CH_3, R^1 = CH_3

17

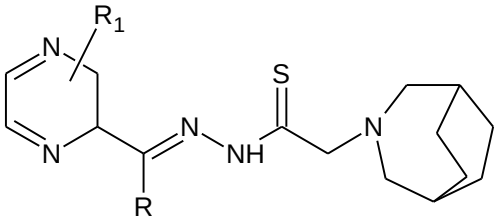

R = CH_3, R^1 = H

R = CH_3, R^1 = 3-CH_3

R = CH_3, R^1 = 5-CH_3

18

Very recently, Hu and co-workers reported synthesis of ten liquiritigenin thiosemicarbazone derivatives (**19**) and their antitumour activities against five cell lines (K562, DU-145, SGC-7901, HCT-116, Hela). Most of the prepared compounds displayed the selective cytotoxicity toward K562 and DU-145 cell lines. Based on the structure-activity relationship (SAR) analysis, it has been concluded that the introduction of thiosemicarbazone at 4-position in liquiritigenin is associated with enhanced cytotoxic activity (Hu, Yang, Pan, Xu, & Ren, 2010).

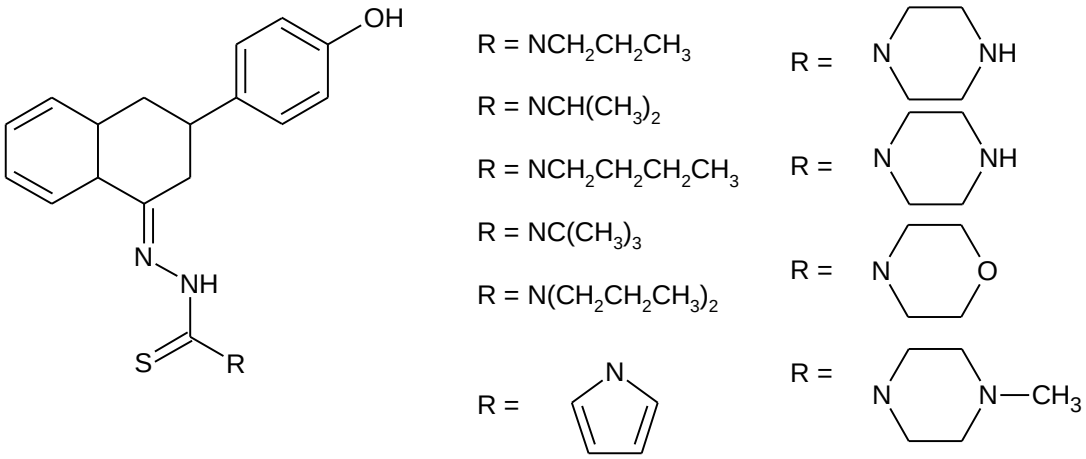

19

To date, the most significant progress in the treatment of cancer has been made with 3-aminopyridine-2-carboxaldehyde TSC (**20**) which has undergone phase II clinical trials. The biological activity of organometallic derived TSC and their metal complexes remains unexplored and this work would in some ways contribute to its development.

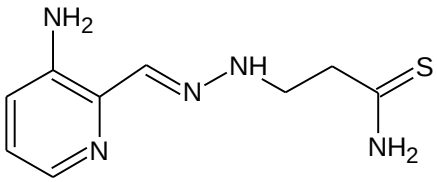

20

1.4 Objectives

The objectives of this study were:

1. To synthesise and characterise a series of zinc(II) ferrocenylthiosemicarbazone complexes derived from thiosemicarbazide, 4-methyl-3-thiosemicarbazide, 4-ethyl-3-thiosemicarbazide and 4-phenyl-3-thiosemicarbazide.

2. To study DNA binding behaviour and nuclease activity of the zinc(II) complexes.

2 EXPERIMENTAL

2.1 Materials and measurements

All the reagents and chemicals were obtained from commercial sources (Acros Chemicals, Aldrich) and used as such. Supercoiled (SC) pBR 322 DNA and loading dye were purchased from Fermentas. Ultrapure water (18.2 MΩ.cm) was obtained from a Barnstead water purification unit. Calf thymus (CT) DNA, agarose (molecular biology grade) and ethidium bromide (EB) were from Sigma. The elemental analysis was carried out using Perkin–Elmer 2400 series-11 CHN/O analyser. The infrared, electronic and fluorescence spectra were recorded on Perkin–Elmer 2000, Perkin Elmer-Lambda 35 and Jasco FP-750 spectrophotometers respectively. Molar conductivity measurements were made using a Eutech Con 510 conductivity meter. Cyclic voltammetric measurements were done on a BAS-Epsilon electrochemical system using a three electrode set-up comprising of a platinum disc working, platinum wire auxiliary and an Ag/AgCl reference electrode. Tetrabutylammonium hexafluorophosphate ($TBAPF_6$) (0.1 M) was used as a supporting electrolyte in acetonitrile.

2.2 X-ray crystallography

Determination of cell constant and data collection were carried out at 100.0(1) K using the Oxford Cryosystem Cobra low-temperature attachment with Mo-Kα radiation (λ = 0.71073 Å) on Bruker SMART APEXII CCD area-detector diffractometer equipped with a graphite monochromator. The data were reduced using SAINT. A semi-empirical absorption correction was applied to the data using SADABS. The structures were solved by direct methods and refined against F^2 by full-matrix least-squares using SHELXTL. All hydrogen atoms were positioned

geometrically and were refined using a riding model whereas non-hydrogen atoms were refined anisotropically.

2.3 DNA binding

2.3.1 Preparation of reagents

To prepare Tris HCl (5 mM Tris-HCl, 50 mM NaCl, pH 7.1) buffer for titrations, 0.0785 g (0.5 mmol) of Tris HCl was dissolved in 85 mL of ultra pure water with constant stirring. To this solution (0.2922 g, 5 mmol) of NaCl salt was added and the solution was stirred to have complete dissolution. The pH of the buffer solution was then adjusted to pH 7.1 by adding small aliquots of 1M HCl. The final volume of the solution was adjusted to 100 mL using ultra pure water. The final pH of the solution was then confirmed with the pH meter. The Tris HCl solution was prepared fresh before each experiment and not used for more than 2 − 3 days. The pH of the Tris HCl buffer solution was constantly verified before each titration. To prepare CT DNA solution, approximately 0.05 g of CT DNA was dissolved in 50 mL Tris HCl buffer and constantly stirred overnight to ensure complete dissolution. The resulting solution was then filtered through a 0.2 μm nylon filter. Precautions were taken to avoid contamination of the DNA by other biological materials. Solutions of CT DNA were prepared fresh before each experiment and not used more than 2 days. The concentration of DNA solution expressed in moles was determined by UV-visible spectrophotometer. The absorbance of the resulting filtered DNA solution was measured against Tris HCl buffer as blank in the range of 200 − 800 nm. When DNA is isolated from organisms, usually there remains protein present in the DNA solution; protein is tightly bound to DNA and complete removal of protein is not always possible. To calculate the concentration and purity of the DNA solution, the absorbance of UV light is measured in a spectrophotometer. Both

protein and DNA absorb UV light, except they have different absorbance curves. The peak of light absorption for DNA is at 260 nm and for protein at 280 nm. The solution of CT DNA in the buffer gave a ratio of UV absorbance at 260 and 280 nm of 1.8 − 1.9 : 1 for all the stock solutions of DNA prepared indicating that the DNA was sufficiently free of protein (Reichmann, Rice, Thomas, & Doty, 1954). Therefore no further purification was attempted. The DNA concentration per nucleotide was determined using the molar absorption coefficient of 6600 M^{-1} cm^{-1} at 260 nm.

2.3.2 Absorption spectral titration

For absorption titration, the spectrum was recorded in the range of 200 – 800 nm. The UV-vis scan rate was set to 600 nm/min, and the data interval as 1 nm. The titrations were performed in quartz cuvettes with 10 mm pathlength. The absorption titrations of ligands or metal complexes were performed using a fixed concentration of compound to which increments of the DNA solution were added. The sample cuvette was filled with 3 mL of the ligand or metal complex solution and the reference cuvette with 3 mL of Tris buffer. Both the cuvettes were left in the spectrophotometer and an equal amount of DNA solution was added to both the compound solution and the reference solution. The solutions were allowed to equilibrate for 10 minutes before the next addition. The sequence of addition of DNA, equilibration for 10 minutes and measurement of the spectra were repeated for 6 additions.

2.3.3 Fluorescence spectral titration

For fluorescence titration, all the samples were excited at their respective absorption maxima (λ_{max}) and the emission were observed at *ca*. 410 nm. The

excitation slit width was set as 5 nm while the emission slit width was set to 10 nm. The average time interval was set to 1 second and the data interval to 2.00 nm yielding a scan rate of 120 nm/s. The titrations of ligands or metal complexes were performed using a fixed concentration of compound to which increments of the DNA solution were added. The sample quvette was filled with 3 mL of the ligand or metal complex solution and 50 μl of DNA solution was added. The solution was allowed to equilibrate for 2 minutes before next addition. The sequence of addition of DNA, equilibration for 2 minutes and measurement of the spectra were repeated for 5 additions.

2.3.4 Viscosity measurements

Viscosity measurements were made using Cannon Manning Semi-Micro viscometer. The viscometer was thermostated at 30 ^{o}C in a constant temperature bath. The flow time of a series of DNA solutions (40 μM) containing varying concentrations of metal complex were measured manually using a digital stopwatch. The flow time of the Tris HCl buffer also measured. Data were presented as $(\eta/\eta_0)^{1/3}$ versus the ratio of the concentration of the complex and DNA, where η is the viscosity of DNA in the presence of complex and η^0 is the viscosity of DNA alone. Viscosity values were calculated from the observed flowing time of DNA-containing solutions (t) corrected for that of the buffer alone (t_0), $\eta = (t - t_0)/t_0$.

2.4 DNA cleavage experiments

The cleavage of supercoiled pBR322 DNA (0.5 μg/μl) was studied by agarose gel electrophoresis. To prepare agarose gel, 0.4 g of agarose was added to 40 mL of TAE buffer and the mixture was heated in a microwave oven to boil. The solution obtained was cooled in water bath to 60 ^{o}C before being poured into a gel

mould. A gel comb was placed at one end of the mould. After 30 minutes, the solution transformed into a gel and the comb was removed. In cleavage reactions, supercoiled DNA was treated with solutions of metal complexes (concentrations given in the figure captions). The samples were incubated at 37 ^{o}C for 2 h, under an argon atmosphere in the dark (*i.e.,* in apparatus that was wrapped in an aluminium foil). Each sample was added loading dye and the solution was loaded on agarose gel with a running time of 1 h at a constant voltage of 50 V. The resultant DNA bands after the electrophoresis step were stained with ethidium bromide before being photographed under UV light.

2.5 Preparation of ferrocenylthiosemicarbazone ligands

Ferrocene-1-carbaldehyde thiosemicarbazone, **HFTSC** (**I**)

To a stirred suspension of thiosemicarbazide (0.213 g, 2.336 mmol) in water (40 mL) a few drops of 36% hydrochloric acid (wt% in H_2O) and ferrocenecarboxaldehyde (0.499 g, 2.336 mmol) were added. The resulting mixture was stirred for 4 h at room temperature. The precipitate formed was filtered off, washed with water and dried in vacuum over silica gel to yield an orange powder (0.23 g, 80%). Mp: 175 – 177 ^{o}C. Calculated for $C_{12}H_{13}N_3SFe$: C, 50.19; H, 4.56; N, 14.63%. Found: C, 50.16; H, 4.73; N, 14.44. IR data (KBr, cm^{-1}): 3430, 3279, 3144, ν(N–H); 1600, ν(C=N); 840, ν(C=S). UV-vis in aqueous DMF (10% DMF) [λ_{max}, nm (ε, M^{-1} cm^{-1})]: 265 (11322), 306 (22882), 454 (1038).

All other thiosemicarbazone ligands were made similarly using the appropriate thiosemicarbazides. The ligands were obtained as orange (**HFMTSC, HFETSC)** or red (**HFPTSC)** powder.

Ferrocene-1-carbaldehyde 4-methylthiosemicarbazone, **HFMTSC** (**II**)

This compound was made from 4-methyl-3-thiosemicarbazide (0.246 g, 2.336 mmol). Yield: 0.256 g, 85%. Mp: 135 – 136 ^{o}C. Calculated for $C_{13}H_{15}N_3SFe$: C, 52.14; H, 5.20; N, 13.95%. Found: C, 52.31; H, 5.29; N, 13.72. IR data (KBr, cm^{-1}): 3370, 3300, 3255, 3136, ν(N–H); 1602, ν(C=N); 850, ν(C=S). UV-vis in aqueous DMF (10% DMF) [λ_{max}, nm (ε, M^{-1} cm^{-1})]: 263 (12235), 308 (23489), 454 (773).

Ferrocene-1-carbaldehyde 4-ethylthiosemicarbazone, **HFETSC** (**III**)

This compound was made from 4-ethyl-3-thiosemicarbazide (0.278 g, 2.336 mmol). Yield: 0.293 g, 93%. Mp: 144 – 146 ^{o}C. Calculated for $C_{14}H_{17}N_3SFe$: C, 53.35; H, 5.44; N, 13.33%. Found: C, 53.67; H, 5.71; N, 13.12. IR data (KBr, cm^{-1}): 3363, 3150, ν(N–H); 1603, ν(C=N); 827, ν(C=S). UV-vis in aqueous DMF (10% DMF) [λ_{max}, nm (ε, M^{-1} cm^{-1})]: 263 (14764), 308 (26571), 460 (1700).

Ferrocene-1-carbaldehyde 4-phenylthiosemicarbazone, **HFPTSC** (**IV**)

This compound was made from 4-phenyl-3-thiosemicarbazide (0.390 g, 2.336 mmol). Yield: 0.331 g, 91%. Mp: 190 – 192 ^{o}C. Calculated for $C_{18}H_{17}N_3SFe$: C, 59.52; H, 4.72; N, 11.57%. Found: C, 59.32; H, 4.60; N, 11.57. IR data (KBr, cm^{-1}): 3345, 3314, 3124, ν(N–H); 1601, ν(C=N); 830, ν(C=S). UV-vis in aqueous DMF (10% DMF) [λ_{max}, nm (ε, M^{-1} cm^{-1})]: 266 (15151), 312 (21977), 460 (1603).

2.6 Preparation of zinc complexes

Bis(ferrocenecarbaldehyde thiosemicarbazonato)zinc(II), **Zn(FTSC)$_2$ (V)**

$Zn(CH_3COO^-)_2.2H_2O$ (0.21 g,1 mmol) dissolved in methanol (60 mL) was added dropwise at room temperature to a mixture of **HFTSC** (0.29 g, 1 mmol) and KOH (0.12 g, 2 mmol) in methanol (15 mL). Amorphous orange solids separated out immediately. The suspension was stirred under reflux for 4 h and filtered. Allowing the filtrate to evaporate slowly at room temperature gave the product as brown crystals (0.252 g, 79%). These crystals were suitable for X-ray crystallography. Mp: >230 ^oC (dec). Calculated for $C_{24}H_{24}N_6S_2Fe_2Zn$: C, 45.20; H, 3.79; N, 13.18%. Found: C, 45.08; H, 3.48; N, 12.79. IR data (KBr, cm^{-1}): 3453, 3344, ν(N–H); 1596, ν(C=N); 834, ν(C−S). UV-vis in aqueous DMF (10% DMF) [λ_{max}, nm (ε, M^{-1} cm^{-1})]: 265 (23734), 306 (44613), 460 (2427). Molar conductivity (10^{-3} M, DMF): 2.3.

All other complexes were made similarly using the appropriate thiosemicarbazone ligands. The complexes were obtained as brown crystals (diffraction grade).

Bis(ferrocenecarbaldehyde 4-methylthiosemicarbazonato)zinc(II) Monomethanol, **Zn(FMTSC)·CH$_3$OH (VI)**

This compound was made from **HFMTSC** (0.30 g, 1 mmol). Yield: 0.29 g, 83%. Mp: >230 ^oC (dec). Calculated for $C_{27}H_{32}Fe_2N_6OS_2Zn$: C, 46.48; H, 4.62; N, 12.04%. Found: C, 46.10; H, 4.58; N, 12.36. IR data (KBr, cm^{-1}): 3368, ν(N–H); 1601, ν(C=N); 835, ν(C−S). UV-vis in aqueous DMF (10% DMF) [λ_{max}, nm (ε, M^{-1} cm^{-1})]: 262 (28785), 308 (53067), 458 (2714). Molar conductivity (10^{-3} M, DMF): 2.4 S cm^2 mol^{-1}.

Bis(ferrocenecarbaldehyde 4-ethylthiosemicarbazonato)zinc(II), **Zn(FETSC)** (**VII**)

This compound was made from **HFETSC** (0.32 g, 1 mmol). Yield: 0.281 g, 81%. Mp: >230 ^{o}C (dec). Calculated for $C_{28}H_{32}N_6S_2Fe_2Zn$: C, 48.47; H, 4.65; N, 12.11%. Found: C, 48.12; H, 4.29; N, 11.71. IR data (KBr, cm^{-1}): 3339, ν(N–H); 1601, ν(C=N); 820, ν(C−S). UV-vis in aqueous DMF (10% DMF) [λ_{max}, nm (ε, M^{-1} cm^{-1})]: 262 (25309), 308 (44736), 457 (3068). Molar conductivity (10^{-3} M, DMF): 3.3 S cm^2 mol^{-1}.

Bis(ferrocenecarbaldehyde 4-phenylthiosemicarbazonato)zinc(II) Monohydrate, **Zn(FPTSC)·H_2O** (**VIII**)

This compound was made from **HFPTSC** (0.36 g, 1 mmol). Yield: 0.311 g, 77%. Mp: >230 ^{o}C (dec). Calculated for $C_{36}H_{34}Fe_2N_6OS_2Zn$: C, 53.52; H, 4.24; N, 10.40%. Found: C, 53.51; H, 4.41; N, 10.01. IR data (KBr, cm^{-1}): 3319, ν(N–H); 1601, ν(C=N); 828, ν(C−S). UV-vis in aqueous DMF (10% DMF) [λ_{max}, nm (ε, M^{-1} cm^{-1})]: 266 (28766), 320 (39530), 446 (1423). Molar conductivity (10^{-3} M, DMF): 2.1 S cm^2 mol^{-1}.

3 RESULTS AND DISCUSSION

3.1 Synthesis and General Aspects

The ferrocenylthiosemicarbazone ligands **HFTSC** (**I**), **HFMTSC** (**II**), **HFETSC** (**III**) and **HFPTSC** (**IV**) were prepared following published procedure (Casas *et al.*, 2004), by a reaction of ferrocenecarboxaldehyde with corresponding thiosemicarbazide in the presence of HCl as a catalyst at room temperature (Scheme 1.2). They are stable in solid state, but start to decompose in solution (darkening) if left for 3 days under normal laboratory conditions.

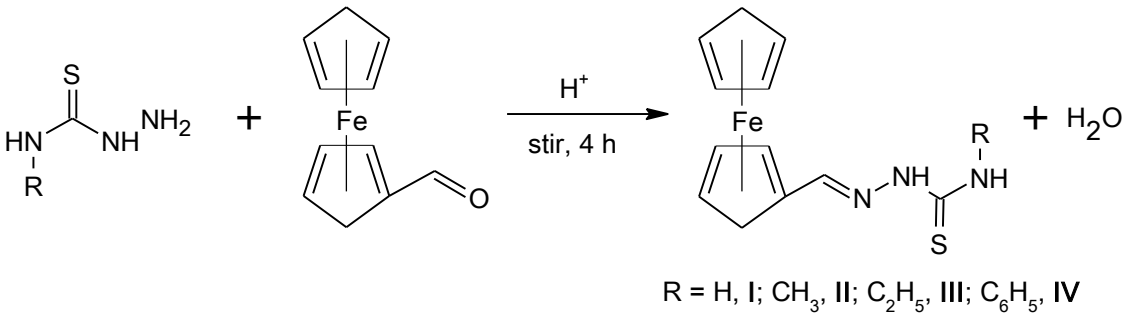

Scheme 3.1: General synthesis of ferrocenylthiosemicarbazone ligands.

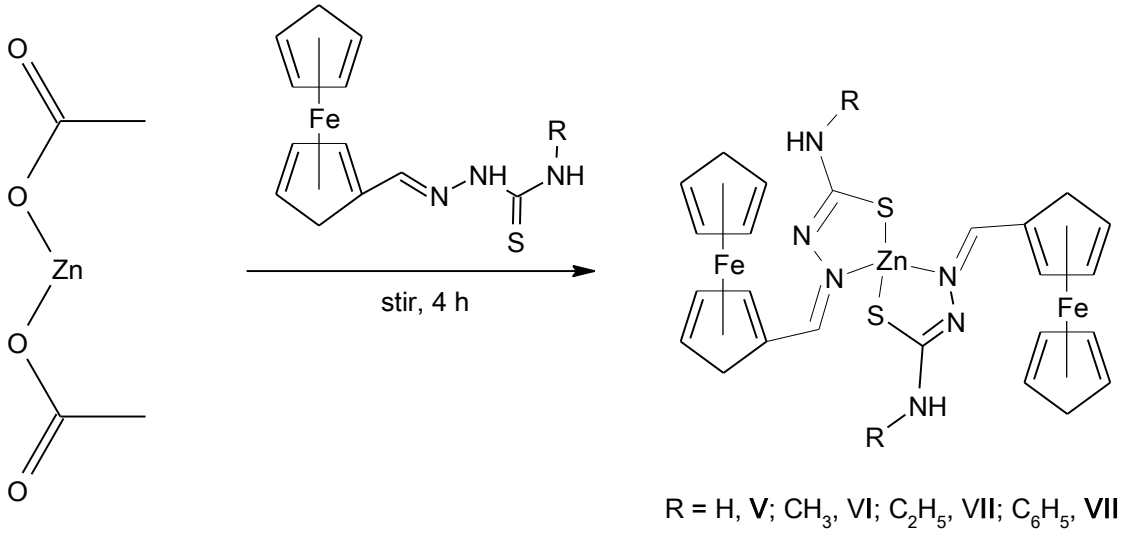

Scheme 3.2: General synthesis of zinc complexes.

The new zinc complexes **Zn(FTSC)$_2$** (**V**), **Zn(FMTSC)$_2$·CH$_3$OH** (**VI**), **Zn(FETSC)$_2$** (**VII**) and **Zn(FPTSC)$_2$·H$_2$O** (**VIII**) have been isolated from

methanolic solutions containing dihydrated zinc(II) acetate as the starting material (Scheme 3.2). All the complexes were obtained in good yields (>75%) and characterised by elemental analysis, FT-IR, UV-vis and cyclic voltammetry. They are soluble in acetone, acetonitrile (except complex **V**), DMF and DMSO and did not exhibit decomposition in 10% aqueous DMF after 3 h incubation at 37 ^{o}C (monitored by UV-vis spectroscopy). The molar conductivity values were in the range 2.3 to 3.3 S cm^{-2} mol^{-1} (Table 3.1) indicating that these complexes are non-electrolytes (Geary, 1971). The electronic spectra of the complexes in aqueous DMF showed a ferrocene-centred band at *ca*. 455 nm and, the remaining ligand-centred bands in the UV region. In the infrared spectra of the complexes, the number of bands corresponding to ν(N−H) vibrations has decreased compared to those of the free ligands owing to deprotonation (Calatayud, LÃ³pez-Torres, & Mendiola, 2007). The energy of these bands is shifted to higher energy relative to those in the spectra of the free ligands. However, the shifts (either to lower energy or higher energy) observed in the bands assigned to ν(CN) and ν(CS) are found to be insignificant. The structures of the complexes have been revealed by single crystal X-ray crystallography.

Table 3.1: Selected physicochemical data for the zinc complexes.

	IR[a]/cm^{-1} [ν(CN), [νCS]	Visible spectra band[b] λ_{max} (ε/M^{-1} cm^{-1})	Molar conductance Λ_M[c]/ S cm^{-2} mol^{-1}
V	1596, 834	460 (2427)	2.3
VI	1601, 835	458 (2714)	2.4
VII	1601, 820	457 (3068)	3.3
VIII	1601, 828	446 (1423)	2.1

[a] In KBr
[b] In aqueous DMF (9:1 v/v)
[c] Molar conductivity in DMF